International Journal of Applied Engineering Research ISSN 0973-4562 Volume 14, Number 6 (2019) pp. 1324-1333

Removal of malachite green and toluidine blue dyes from aqueous solution using a clay-biochar composite of bentonite and sweet sorghum bagasse

Fosso-Kankeu E.*, Potgieter J., Waanders F.B.

Water Pollution Monitoring and Remediation Initiatives Research Group,
School of Chemical and Minerals Engineering, North West University, South Africa.

Abstract

A clay-biochar composite was prepared through slow pyrolysis of a mixture of bentonite clay and sweet sorghum bagasse. The adsorption of cationic dyes, namely, toluidine blue (TB) and malachite green (MG), by the clay-biochar composite was investigated to determine the adsorption mechanism and its sorption potential. Bentonite clay, sweet sorghum biochar and the bentonite-biochar composite were characterized through X-ray fluorescence (XRF), scanning electron microscopy (SEM) and Fourier transform infrared (FT-IR) analyses. For the adsorption study, the effects of exposure time, initial dye concentration and temperature were investigated. The findings clearly illustrated the complex physico-chemical properties of the clay-biochar composite encompassing distinct features of bentonite clay and biochar, therefore confirming successful preparation. The adsorption of MG was found to occur on a heterogeneous surface as predicted by the Freundlich isotherm model, while the adsorption of TB occurred mostly at a monolayer surface described by the Langmuir isotherm model. The adsorption equilibrium data was best described by the pseudo-second order kinetic model for all adsorbents. The estimated adsorption capacity of the clay-biochar composite (12.1255 mg/g for MG and 9.9356 mg/g for TB) suggests improved adsorption capacity of the biochar after incorporation of clay. The thermodynamic study revealed that the adsorption of dyes was mostly a spontaneous and exothermic process.

The adsorbent investigated in this study showed good potential for the removal of cationic dyes from aqueous solution and could be considered for the remediation of water polluted by industrial effluents.

Keywords: Clay-biochar composite, cationic dyes, water pollution, adsorption, kinetic, isotherm, thermodynamic

1 Introduction

The shortage of fresh water around the world is exacerbated by pollution deriving mostly from industrial activities. Some of these pollutants discharged in the environment are very recalcitrant and could persist in the environment for several years and cause serious harm to the surrounding biota. Such pollutants include synthetic dyes, which are extensively used by the food processing, dyeing, textile, cosmetics, leather, printing, electroplating, distillation and pharmaceutical industries [1-4].

The main culprit in the discharge of dyes into receiving surface waters is the textile industry. Of the 7 x 10^5 tons of dyes consumed every year in the dyeing process by the textile industry, it is reported that approximately 10 – 15% are directly released into water systems [5-10]. Examples of dyes used in the textile industry include, but are not limited to, acid dyes, basic dyes, direct dyes, mordant dyes, reactive dyes, disperse dyes, sulphur dyes and vat dyes.

High concentrations of coloured dyes entering the surface water system colourize the water and impede light penetration, eventually inhibiting photosynthetic activity and adversely affecting aquatic life [1, 11]. Depending on their concentration in water, dyes can have an acute or chronic effect on organisms; bath exposure to dyes is known to lead to problems such as dermatitis, cancer, mutation, allergy and skin irritation in humans [1, 12, 13]. According to Vadivelan and Kumar [14], acute exposure to methylene blue dye may significantly affect the health of human beings, causing symptoms such as cyanosis, jaundice, shock, vomiting, increased heart rate, tissue necrosis, quadriplegia and Heinz-body formation. The negative impact of dyes on the aesthetics and sustainability of biota in receiving fresh water (as well as possible risk to human health) has prompted governments around the world to regulate the discharge of dyes in industrial effluents, therefore compelling industries to remove dyes from their effluents prior to discharge in the environment.

Adsorption techniques could be a very attractive method of removal due to its ease of application, low energy requirement and worldwide availability of cheap adsorbents, among which are clay and biochar. Bentonite clay is a fundamental soil component that can be found in three major locations in South Africa, namely, the Koppies district in the Free State, Heidelberg district in the Western Cape and Wodehouse district in Northern Natal. Therefore, the use of bentonite clay is not only effective but also very economical. The clay has a very large surface area, especially if it is hydrated in water. The microscopic platelets of bentonite clay are negatively charged on the flat surfaces, while the edges of the platelets are positively charged [15]. Bentonite clay has a 2:1 layered structure and consists of an alumina octahedral layer between two silica tetrahedral layers [16].

Biochar can be produced from several types of raw materials such as rice husk [17], pine needles [18], loblolly pine chips [19], anaerobic digestion residues, palm bark and eucalyptus [20], soybean stover and peanut shells [21], or corn stover and apple wood [22]. Although the production conditions can

affect the physical, chemical and mechanical properties, biochar generally has oxygen-containing groups such as hydroxyl (OH), carboxylates (-COO^- and -COH) and a net negative charge [23-25], which makes it a suitable adsorbent for the removal of pollutants from wastewaters.

The adsorption potential of clay and biochar can be enhanced through the synthesis of a composite of the two materials. The biochar has a good porous structure and required functional groups [26, 27], while adding clay to biochar increases the surface area and exchange capacity, thereby improving the adsorption capacity. This study considers (for the first time to the best of our knowledge) application of a clay-biochar composite for removal of the cationic dyes toluidine blue and malachite green from aqueous solution.

2 METHODS

2.1 Materials

The two cationic dyes, namely, malachite green (triarylmethane dye) and toluidine blue (basic thiazine metachromatic dye), were purchased from Merck Millipore and Sigma Aldrich (South Africa), respectively. The bentonite clay was mined close to the small town Koppies in the Free State Province of South Africa. Due to its availability, sweet sorghum bagasse was chosen as the source of biomass for biochar.

2.2 Preparation of adsorbents

The biochar and the clay-biochar composite were prepared as described in our previous report [26]. Briefly, the biochar was produced from sweet sorghum bagasse through slow pyrolysis, while the clay-biochar composite was produced by adding sweet sorghum bagasse to a slurry of bentonite clay; the mixture was dried before undergoing slow pyrolysis.

2.3 Characterization of adsorbents

An X-ray fluorometer (XRF) MagiX PRO & SuperQ Version 4 was used to chemically analyse the prepared adsorbents, while a Fourier transform infrared (FT-IR) spectrometer (Shimadzu) was used to identify the binding groups at the surface of the adsorbents that were likely to be involved in the adsorption process.

The surface morphology of the adsorbents was determined using a scanning electron microscope (SEM) TECSAN, model VEGA 3 XMU (Czech Republic) equipped with a 10-micron lens, integrated with an energy dispersive X-ray.

2.4 Adsorption experiments

The adsorption potential of bentonite clay, sweet sorghum biochar and the bentonite-biochar composite was investigated in a batch system under fixed conditions, namely solution volume (100 mL), adsorbent dosage (0.5 g) and shaking speed (160 rpm). Parameters such as time, initial concentration and temperature were varied to study the adsorption kinetics, isotherms and thermodynamics, respectively. The time was therefore varied from 10 to 120 mins, with an increment of 10; the initial dye concentrations were 10, 20, 30, 40, 60, 70, 80 and 100 mg/L, and the temperatures were 35, 45 and 55 °C. After adsorption, the mixture was centrifuged at 4000 rpm for 5 mins to separate the loaded adsorbent from the suspended dye, and then the supernatant was collected and analysed using the UV mini-1240 UV-VIS spectrophotometer to determine the concentration of the non-adsorbed dye.

2.5 Adsorption models

2.5.1 Adsorption capacity

The potential of an adsorbent can be estimated by determining its adsorption capacity, which is the amount of adsorbate adsorbed per unit mass of the adsorbent [28]:

$$q_i = \frac{(C_o - C_i)V}{m}\ ;\ \ i = e, \tag{1}$$

where q_i is the amount of dye adsorbed per unit mass of adsorbent (mg/g); C_o is the initial dye concentration in the solution (mg/L); C_i is the dye concentration (mg/L); m is the amount of adsorbent (g) and V is the solution volume (L). The subscript "i" denotes the state of the system either at equilibrium (e) or at a particular time (t).

2.5.2 Isotherms

The Langmuir and Freundlich isotherms were used to model the adsorption of dyes. The equations for these models have been described elsewhere [29].

2.5.3 Kinetic modelling

The adsorption kinetic model describes the rate of sorbate binding at the surface of adsorbent, which is information needed to design wastewater treatment plants. Two kinetic models, namely, pseudo-second-order and pseudo-first-order, were considered to assess the adsorption rate of the dyes onto the respective adsorbents. These models are expressed by equations described in previous studies [32, 33, 34]

2.5.4 Thermodynamic assessment

The impact of temperature on the dye adsorption process was assessed by determining thermodynamic parameters such as the standard free energy ($\Delta G^\circ, kJ/mol$), enthalpy change ($\Delta H^\circ, kJ/mol$) and entropy change ($\Delta S^\circ, kJ/mol$).

The Gibbs free energy (ΔG°) is expressed by the following equation:

$$\Delta G^\circ = -RTlnK_c \tag{2}$$

where R is a gas constant [8.314 kJ/(mol K)], T is the solution temperature (K) and K_c is the equilibrium constant which can be obtained from the relation [35]:

$$K_c = \frac{C_a}{C_e} \tag{3}$$

where C_a is the amount of dye adsorbed (mg/L) and C_e is the equilibrium concentration of solution (mg/L).

Following van't Hoff's equation [35]:

$$\ln K_c = \frac{-\Delta G^\circ}{RT} = \frac{-\Delta H^\circ}{RT} + \frac{\Delta S^\circ}{R} \tag{4}$$

The values of ΔH° and ΔS° can be obtained from the slope and intercept of a plot of $ln\ K_c\ vs.\ 1/T$.

3 RESULTS AND DISCUSSION

3.1 Adsorbents properties

3.1.1 XRF analysis

The XRF analysis results of the bentonite clay are summarized in Table 1 and indicate the most prominent compounds on a mass-percentage basis. The dominance of alumina and silicate clearly confirm the nature of bentonite clay as an aluminosilicate. Calcium and potassium are the main exchangeable ions during the adsorption process.

Table 1: Major chemical components of bentonite clay

Component	Weight %
Al_2O_3	18.6775
SiO_2	62.8874
K_2O	2.5794
CaO	1.8175
Fe_2O_3	10.8592

3.1.2 SEM analysis

The morphology of the bentonite clay, biochar and composite was determined using a scanning electron microscope (SEM) at an electron acceleration voltage of 20 kV. Figure 1(a) shows that the bentonite has a porous structure indicating a large surface area. Figure 1(b) shows the biochar exhibits a more crystalline, fibrous structure probably originating from lignocellulosic materials dominant in the initial biomass. In Figure 1(c), the fibrous materials from the biochar are mostly covered with rod-like structures probably deriving from the bentonite, implying that the formation of the biochar-bentonite composite was successful. A similar change of shape was identified in a previous study [36].

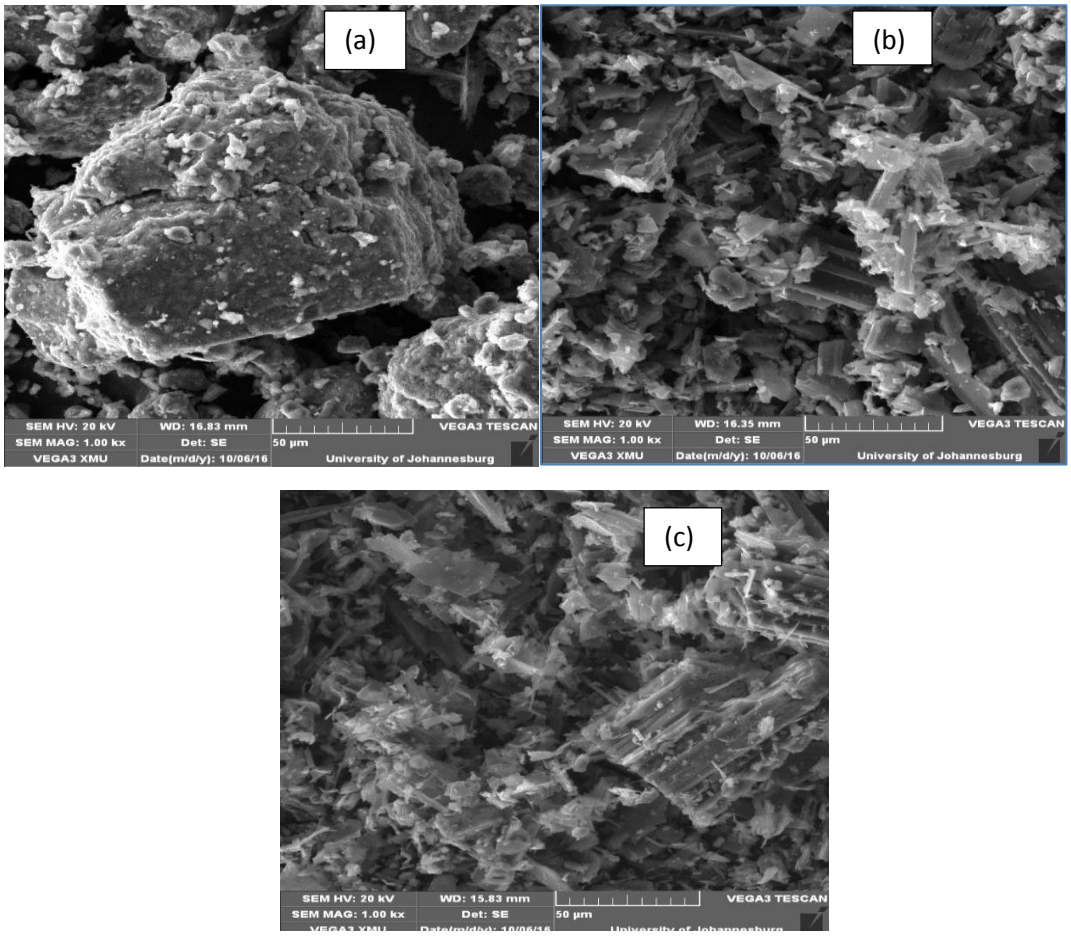

Figure 1: SEM images of bentonite (a), biochar (b) and bentonite-biochar-composite

3.1.3 FT-IR analysis

The FT-IR spectra in Figure 2(a) show that the bentonite and biochar have different binding groups. The bands at 3000, 2850 and 2300 cm^{-1} (which can be ascribed to C=C-H asymmetric stretching vibration, C-H stretching off C=O and CN stretching vibration, respectively) were observed on the biochar spectrum but not on the bentonite spectrum, while the peak of the band at 1600 cm^{-1} corresponding to the binding group C=O stretching vibration is stronger on the spectrum of the biochar than that of the bentonite. However, the band at 1000 cm^{-1} corresponding to the C-O stretching vibration is only observed on the spectrum of the bentonite. All the above bands are present on the spectrum of the composite, further confirming a successful incorporation during the preparation. The binding of toluidine blue and malachite green on the adsorbents resulted in the occurrence or disappearance of binding groups, as shown in Figures 2(b), (c) and (d).

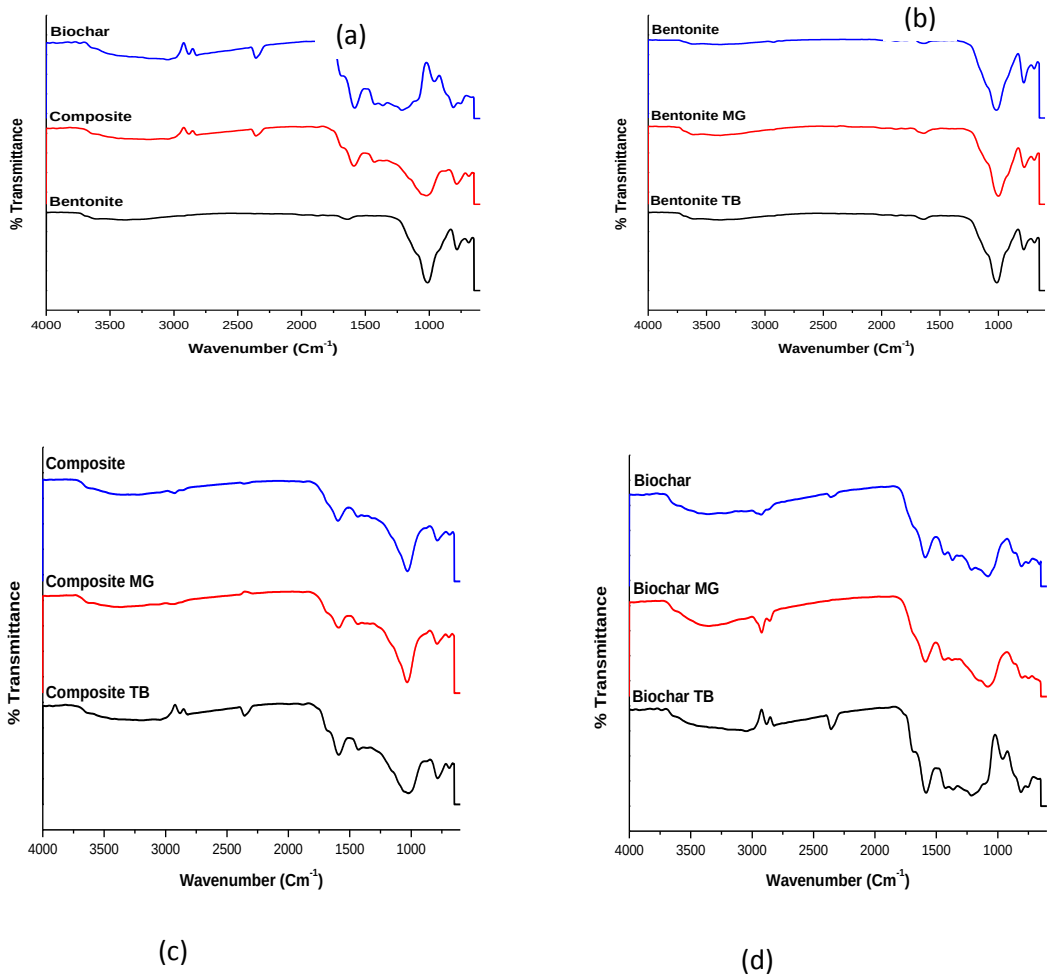

Figure 2: FT-IR spectra of the three adsorbents (a), loaded bentonite (b), loaded composite (c) and loaded biochar (d).

3.2 Adsorption kinetic modelling

The pseudo-first-order and pseudo-second-order kinetic models were used to assess the adsorption behaviour at different initial dye concentrations. The experimental adsorption data fit better with the pseudo-second-order model, which was therefore considered for the prediction of the adsorption behaviour of the adsorbents. The values of $k_i\,; i = 1, 2$ and $q_{e_{cal}}$ were calculated from the intercept $(1/k_i q_e^2)$ and slope $(1/q_e)$ *of* the plot $t/q_t\ vs.\ t$ in Figure3 and Figure 4, respectively, and presented in Table 2 Table 3. The $q_{e_{\exp}}$ was found to be in good agreement with the $q_{e_{cal}}$ for both pseudo-first-order and pseudo-second-order models. The values of R^2 for both kinetic models are relatively close, but higher values of R^2 suggest the applicability of the pseudo-second-order model for adsorption of both MG and TB onto the various adsorbents. Table 2 and Table 3 show that the adsorption capacity $(q_{e(\exp)})$ of the composite is higher than that of the biochar, which implies that the composite has a higher affinity for MG and TB dyes [37, 38]. This indicates that the incorporation of clay resulted in physico-chemical changes that improved the attraction potential of biochar for cationic dyes.

Table 2: Kinetic model parameters for MG adsorption

Adsorbent		Kinetic Model and Parameters			
		Pseudo 1st order		Pseudo 2nd order	
Biochar					
$q_{e(exp)}$ (mg/g)	**9.8400**				
		q_{e1}	9.5953	q_{e2}	10.0616
		k_1	0.1634	k_2	0.0369
		R^2	0.9705	R^2	0.9953
Bentonite Clay					
$q_{e(exp)}$ (mg/g)	**16.6087**				
		q_{e1}	16.5552	q_{e2}	16.5841
		k_1	0.5562	k_2	0.9007
		R^2	0.9997	R^2	0.9999
Composite					
$q_{e(exp)}$ (mg/g)	**12.1255**				
		q_{e1}	11.8973	q_{e2}	12.1788
		k_1	0.2434	k_2	0.0710
		R^2	0.9864	R^2	0.9975

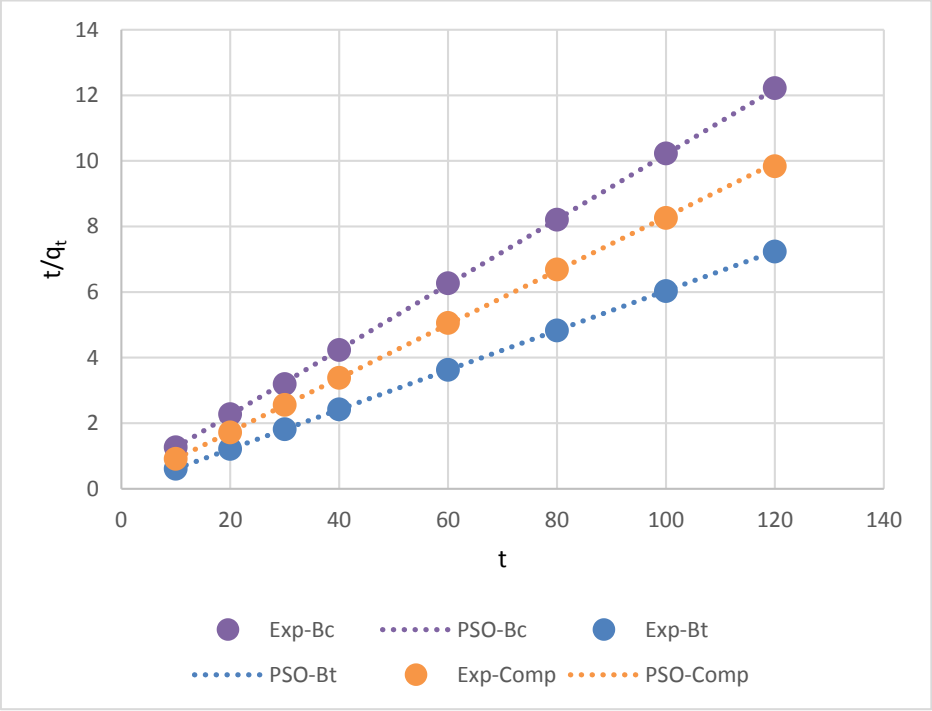

Figure 3: Pseudo-second order kinetic plot for the adsorption of MG

Table 3: Kinetic model parameters for TB adsorption

Adsorbent		Kinetic Model and Parameters			
		Pseudo 1st order		Pseudo 2nd order	
Biochar					
$q_{e(exp)}$ (mg/g)	**9.6480**				
		q_{e1}	9.3845	q_{e2}	9.9461
		k_1	0.1444	k_2	0.0297
		R^2	0.9595	R^2	0.9930
Bentonite Clay					
$q_{e(exp)}$ (mg/g)	**24.9489**				
		q_{e1}	24.8840	q_{e2}	24.9272
		k_1	0.5407	k_2	0.5559
		R^2	0.9998	R^2	0.9999
Composite					
$q_{e(exp)}$ (mg/g)	**9.9356**				
		q_{e1}	9.3719	q_{e2}	9.9460
		k_1	0.1612	k_2	0.0316
		R^2	0.8614	R^2	0.9659

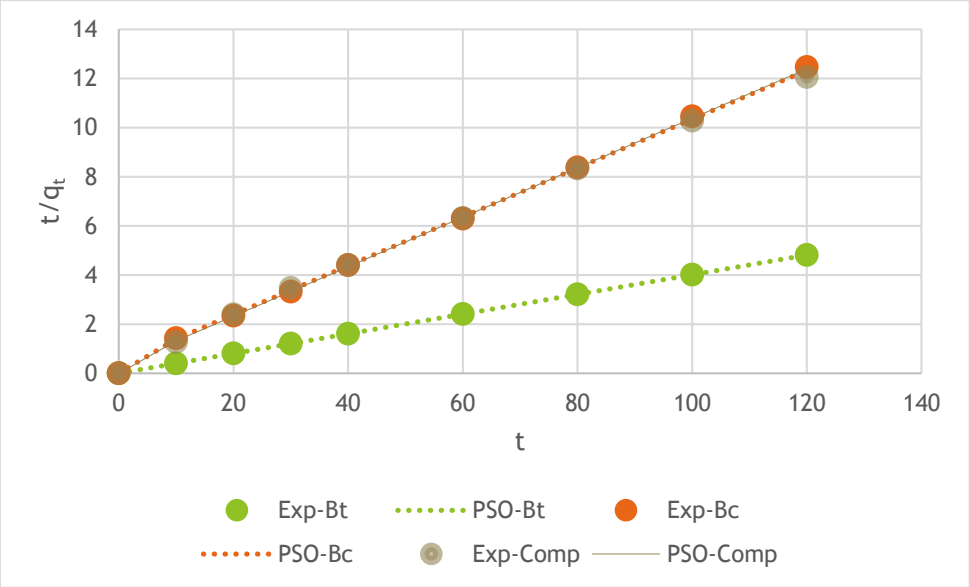

Figure 4 Pseudo-second order kinetic plot for the adsorption of TB

3.3 Adsorption isotherm modelling

The adsorption behaviour of the adsorbents during the removal of toluidine blue and malachite green from solution was assessed using two common adsorption isotherm models, namely, Langmuir and Freundlich. The adsorption capacity increased with the increasing concentration of dye in aqueous solution, implying that the available binding sites were quickly saturated when more dye was present in solution [39]. The adsorption data fit the Freundlich model better than the Langmuir model; therefore, the discussion mainly focuses on the Freundlich model. The isotherm parameters and the coefficients of determination (R^2) for the adsorption of MG and TB are presented in Table 4 and Table 5, respectively.

Table 4: Isotherm model parameters for MG adsorption

Malachite Green Isotherm Study				
Adsorbent	**Best model**	**Model Parameters**		**Adsorption Potential (q_e) (mg/g)**
Bt	Freundlich	kf	121.3520	2834.840
		n	1.2415	
		R^2	0.7840	
Bc	Freundlich	kf	1.9290	4638.388
		n	0.5025	
		R^2	0.9105	
Composite	Freundlich	kf	10.3050	218.701
		n	1.2805	
		R^2	0.9515	

Table 4 clearly shows that the Freundlich isotherm model best describes the adsorption of MG by all adsorbents. The R^2 values obtained for the adsorption of MG by the biochar and the composite were closer to unity, implying that the Freundlich model was suitable only for the prediction of the adsorption of MG on the biochar and the composite. The affinity of the adsorbent for a given dye is indicated by the value of n. Table 4 shows that n > 1 when assessing the adsorption of dyes by the composite, indicating that the adsorbent is effective over the entire range of dye concentrations, and n < 1 when assessing the adsorption of dyes by the biochar, indicating that the adsorbent is effective only for higher concentrations of dyes studied [2].

Table 5: Isotherm model parameters for TB adsorption

Toluidine Blue Isotherm Study				
Adsorbent	**Best model**	**Model Parameters**		**Adsorption Potential (q_e) (mg/g)**
Bt	Langmuir	Q	17.9750	18.418
		K	-0.8310	
		R^2	0.9800	
Bc	Freundlich	kf	0.5317	8.659
		n	1.4020	
		R^2	0.7870	
Composite	Langmuir	Q	9.4885	9.419
		K	2.6975	
		R^2	0.9955	

Table 5 shows that the Langmuir isotherm model best fits adsorption data of two adsorbents, namely, bentonite and composite. The R^2 values obtained from the adsorption of TB by the bentonite and the composite are closer to unity, implying that the Langmuir isotherm is only suitable for the prediction of the adsorption of TB onto the bentonite and the composite, with maximum adsorption capacities of 18.418 and 9.419 mg/g respectively. This implies that the malachite green is mainly adsorbed at the top surface of the composite. The R_L value $[R_L = 1/(1 + bC_0)]$, also known as the separation factor, is a dimensionless constant representing the essential features of the Langmuir isotherm that predicts the favourability of the adsorption process: the adsorption will be unfavourable if $R_L > 1$, favourable if $0 < R_L < 1$, linear if $R_L = 1$ and irreversible if $R_L = 0$ [2, 40]. In these experiments, the R_L value indicates favourable adsorption only when the composite is used as adsorbent ($R_L = 0.038$).

3.4 Thermodynamics predictions

The effect of temperature on MG and TB adsorption was investigated at three different temperatures (35, 45 and 55 °C). The results indicated an influence of temperature on the adsorption of MG onto the adsorbents; however, a consistent trend was observed only when the dyes were adsorbed onto the biochar. The maximum adsorption of MG was achieved at 35° C by biochar, with the adsorption decreasing with increased temperature. These results show the exothermic nature of the adsorption. The weakening of adsorptive forces between active sites of the adsorbents and adsorbate species and between the adjacent molecules of the adsorbed phase may explain the decrease of adsorption capacity with the rise in temperature [35]. The thermodynamic parameters were estimated to evaluate the viability and nature of the adsorption process. The values of ΔH° and ΔS° were obtained from the slope and intercept of the $lnK_c\ vs.\ 1/T$ plot; these values are shown in Table 6. These values were found to be negative; a negative enthalpy implies that the process is exothermic, while a negative entropy implies that the dyes were orderly adsorbed onto the biochar-dye interface. The values of ΔG were negative for the adsorption of toluidine blue onto the biochar, implying that the adsorption process was spontaneous [41], while the adsorption of malachite green onto the biochar at 55 °C was not spontaneous. In general, the values of ΔG increased with increasing temperature, confirming that the adsorption was not favourable at higher temperature.

Table 6: Thermodynamic parameters of the adsorption of TB and MG onto the biochar

Dye	**ΔG° (KJ/mol)**			**ΔH (KJ/mol)**	**ΔS (KJ/mol/K)**
	308 K	**318 K**	**328 K**		
Toluidine	-4945.52	-3363.32	-1780.52	-53720.1	-158.28
Malachite	-7119.25	-2309.27	2500.71	-155338.78	-481

4 CONCLUSION

The results obtained from the characterization of the adsorbents showed that the synthesis of the composite was performed successfully. The composite and the biochar showed good potential for the removal of cationic dyes from the aqueous phase, with the adsorption onto the composite being more favourable, as predicted. The adsorption data for the removal of malachite green from solution fit the Freundlich model, implying that adsorption occurs on the heterogeneous surface, while the adsorption of toluidine blue onto the bentonite clay and the composite could be predicted using the Langmuir model, which suggests binding at a monolayer surface. The adsorption kinetics can be well described by the pseudo-second-order model, implying that the chemisorption mechanism is predominant. The thermodynamic study showed that the adsorption of dyes onto the biochar occurs mostly through a spontaneous and exothermic process. It was found that filling biochar with bentonite clay improved its adsorption capacity. However, a significant improvement could be achieved by increasing the clay/biomass ratio during the preparation of the composite.

Acknowledgements

The authors are grateful to the sponsors from the North-West University and the National Research Foundation (NRF) in South Africa. Any opinion, findings and conclusions or recommendations expressed in this material are those of the authors, and therefore the NRF does not accept any liability in regard thereto. The authors of this paper would like to thank the following individuals for their contributions to this paper: Mr. N. Lemmer of the Chemical Engineering Laboratory of the North-West University, Potchefstroom as well as Mr E. Malenga and Ms N. Baloyi from the University of Johannesburg.

REFERENCES

[1] Bhatnagar, A.; Jain, A.K.: A comparative adsorption study with different industrial wastes as adsorbents for the removal of cationic dyes from water. Journal of Colloids and Interface Science. **281**, 49-55 (2005).

[2] Fosso-Kankeu, E.; Mittal, H.; Mishra, S.B.; Mishra. A.K..: Gum ghatti and acrylic acid based biodegradable hydrogels for the effective adsorption of cationic dyes. Journal of Industrial and Engineering Chemistry. **22**, 171-178 (2015a).

[3] Huang, G.; Sun, Y.; Zhao, C.; Zhao, Y.; Song, Z.; Chen, J.; Ma, S.; Du, J.; Yin, Z.: Water-n-BuOH solvothermal synthesis of ZnAl-LDHs with different morphologies and its calcined product in efficient dyes removal. Journal of Colloids and Interface Science. **494**, 215-222 (2017).

[4] Natarajan, S.; Bajaj, H.C.; Tayade, R.J.: Recent advances based on the synergetic effect of adsorption for removal of dyes from waste water using photocatalytic process. Journal of Environmental Sciences. In Press.

[5] Vandevivere, P.C.; Bianchi, R.; Verstraete, W.: Treatment and reuse of wastewater from the textile wet processing industry: review of emerging technologies. J. Chem. Technol. **72**, 289-302 (1998).

[6] Fu, Y.; Viraraghavan, T.: Fungal decolorization of dye wastewaters: a review. Bioresour. Technol. **79**, 251-262 (2001).

[7] Kwok, W.Y.; Xin, J.H.; Sin, K.M.: Quantitative prediction of the degree of pollution of effluent from reactive dye mixtures. Color Technol. **118**, 174-180 (2002).

[8] Ozsoy, H.D.; Unyayar, A.; Mazmanci, M.A.: Decolourisation of reactive textile dyes Drimarene Blue X3LR and Remazol Brilliant Blue R by Funalia trogii ATCC 200800. Biodegradation. **16**, 195-204 (2005).

[9] Fan, J.; Wang, Y.G.J.; Fan, M.: Rapid decolorization of azo dye methyl orange in aqueous solution by nanoscale zerovalent iron particles. J. Hazard. Mater. **166**, 904-910 (2009).

[10] Dojcinovic, B.P.; Roglic, G.M.; Obradovic, B.M.; Kuraicac, M.M.; Kostic, M.M.; Nesi, J.; Manojlovic, D.D.: Decolorization of reactive textile dyes using water falling film dielectric barrier discharge. Journal of Hazardous Materials. **192**, 763-771 (2011).

[11] Natarajan, T.S.; Natarajan, K.; Bajaj, H.C.; Tayade, R.J.: Study on identification of leather industry waste water constituents and its photocatalytic treatment. Int. J. Environ. Sci. Technol. **10**, 855-864 (2013).

[12] Walsh, G.E.; Bahner, L.H. Environ. Pollut. Ser. A. **21**, 169 (1980).

[13] Ray, P.K. J. Sci. Ind. Res. India. **45**, 370 (1986).

[14] Vadivelan, V.; Kumar, K.V.: Equilibrium, kinetics, mechanism, and process design for the sorption of methylene blue onto rice husk. Journal of Colloid and Interface Science. **286**, 90-100 (2005).

[15] Hamdi, A.M.: Influence of pH and ionic strength on the adsorption of copper and zinc in bentonite clay. Chem. Sci. Trans. **1**(2), 371-381 (2012).

[16] Alvarez-Ayuso, E.; Garcio-Sanchez, A.: Removal of heavy metals from wastewater by natural and Na-exchanged bentonites. Clays Minerals. **51**, 475-480 (2003).

[17] Leng, L.; Yuan, X.; Zeng, G.; Shao, J.; Chen, X.; Wu, Z.; Wang, H.; Peng, X.: Surface characterization of rice husk bio-char produced by liquefaction and application

for cationic dye (Malachite green) adsorption. Fuel. **155**, 77-85 (2015).

[18] Ahmad, M.; Lee, S.S.; Rajapaksha, A.U.; Vithanage, M.; Zhang, M.; Cho, J.S.; Lee, S-E; Ok, Y.S.: Trichloroethylene adsorption by pine needle biochars produced at various pyrolysis temperatures. Bioresour. Technol. **143**, 615-622 (2013).

[19] Park, J.; Hung, I.; Gan, Z.; Rojas, O.J.; Lim, K.H.; Park, S.: Activated carbon from biochar: influence of its physicochemical properties on the sorption characteristics of phenanthrene. Bioresour. Technol. **149**, 383-389 (2013).

[20] Sun, L.; Wan, S.; Luo, W.: Biochars prepared from anaerobic digestion residue, palm bark, and eucalyptus for adsorption of cationic methylene blue dye: characterization, equilibrium and kinetic studies. Bioresource Technology. **140**, 406-413 (2013).

[21] Ahmad, M.; Lee, S.S.; Dou, X.; Mohan, D.; Sung, J-K; Yang, J.E.; Ok, Y.S.: Effects of pyrolysis temperature on soybean stover- and peanut shell-derived biochar properties and TCE adsorption in water. Bioresour. Technol. **118**, 536-544 (2012).

[22] Sun, H.; Hockadav, W.C.; Masiello, C.A.; Zygourakis, K.: Multiple controls on the chemical and physical structure of biomass. Ind. Eng. Chem. Res. **51**, 3587-3597 (2012).

[23] Chun, Y.; Sheng, G.Y.; Chiou, C.T.; Xing, B.S.: 2004. Compositions and sorptive properties of crop residue-derived chars. Environmental Science and Technology. **38**, 4649-4655 (2004).

[24] Inyang, M.; Gao, B.; Pullammanappallil, P.; Ding, W.C.; Zimmerman, A.R.: Biochar from anaerobically digested sugarcane bagasse. Bioresource Technology. **101**, 8868-8872 (2010).

[25] Yuan, J-H.; Xu, R-K.; Zhang, H.: 2011. The forms of alkalis in the biochar produced from crop residues at different temperatures. Bioresource Technology. **102**(3), 3488-3497 (2011).

[26] Fosso-Kankeu, E.; Waanders, F.B.; Steyn, F.W.: Removal of Cr(VI) and Zn(II) from an aqueous solution using an organic-inorganic composite-biochar-hematite. Desalination and Water Treatment. **59**, 144-153 (2017).

[27] Fosso-Kankeu, E.; Mittal, H.; Marx, S.; Ray, S.S.: Hydrogel-Based Bioflocculants for the Removal of Organic Pollutants from Biodiesel Wastewater. J. Polym. Environ. **25**(3), 844-853 (2016).

[28] Donat, R.; Akdogan, A.; Erdem, E.; Cetisli, H.: Thermodynamics of Pb^{2+} and Ni^{2+} adsorption onto natural bentonite from aqueous solutions. Journal of Colloid and Interface Science. **286**(1), 43-52 (2005).

[29] Fosso-Kankeu, E.; Waanders, F.; Fraser, F.: Bentonite clay adsorption affinity for anionic and cationic dyes. 6th International Conference on Green Technology, Renewable Energy and Environmental Engineering (ICGTREEE'2014). 27-28 November 2014, Cape Town-South Africa. Editors: Muzenda E. and Sandhu S. ISBN: 978-93-84468-08-8. Pp 257-260 (2014).

[30] Yao, Y.; Gao, B.; Fang, J.; Zhang, M.; Chen, H.; Zhou, Y.; et al.: Characterization and environmental applications of clay–biochar composites. Chemical Engineering Journal. **242**, 136-143 (2014).

[31] Mittal, H.; Fosso-Kankeu, E.; Mishra, S.B.; Mishra, A.K.: Biosorption potential of Gum ghatti-g-poly (acrylic acid) and susceptibility to biodegradation by B. subtilis. International Journal of Biological Macromolecules. **62**, 370-378 (2013).

[32] Ruan, Z-H.; Wu, J-H.; Huang, J-F.; Lin, Z-T.; Li, Y-F.; Liu, Y-L.; et al.: Facile preparation of rosin-based biochar coated bentonite for supporting α-Fe 2 O 3 nanoparticles and its application for Cr (vi) adsorption. Journal of Materials Chemistry A. **3**(8), 4595-4603 (2015).

[33] Fosso-Kankeu, E.; Waanders, F.; Fourie, C.L.: Adsorption of Congo Red by surfactant-impregnated bentonite clay. Desalination and Water Treatment. doi: 10.1080/19443994.2016.1177599, 1-9 (2016a).

[34] Weber Jr., W.J.; Morris, J.C.: Journal of Sanitary Engineering Division: AmericanSociety of Civil Engineers. **89**, 31–59 (1963).

[35] Abdelwahab, O.; Fouad, Y.O.; Amin, N.K.; Mandor, H.: Kinetic and thermodynamic aspects of cadmium adsorption onto raw and activated guava *(Psidium guajava)* leaves. Environmental Progress & Sustainable Energy. **34**(2), 351-358 (2015).

[36] Fosso-Kankeu, E.; Waanders, F.B.; Steyn, F.W.: The Preparation and Characterization of Clay-Biochar Composites for the Removal of Metal Pollutants. 7th International Conference on Latest Trends in Engineering and Technology (ICLTET' 2015), November 26-27, 2015 Irene, Pretoria (South Africa). Editors: E. Muzenda and T Yingthawornsuk. ISBN: 978-93-84422-58-5, (2015b).

[37] Fosso-Kankeu, E.; Mulaba-Bafubiandi, A.F.; Mamba, B.B.; Barnard, T.G.: Prediction of metal-adsorption behaviour in the remediation of water contamination using indigenous microorganisms. Journal of Environmental Management, **92**(10), 2786-2793 (2011).

[38] Fosso-Kankeu, E.; Waanders, F.; Maloy, E.: Copolymerization of ethyl acrylate onto guar gum for the adsorption of Mg(II) and Ca(II) ions. Desalination and Water Treatment. doi: 10.1080/19443994.2016.1165147: 1-10, (2016b).

[39] Wang, J.; Chen, C.: Biosorbents for heavy metal removal and their future. Biotechnol. Adv. **27**, 195-226 (2006).

[40] Pandey, S.; Mishra, S.B.: Microwave synthesized xanthan gum-g-poly(ethylacrylate): An efficient Pb^{2+} ion binder. Carbohydrate Polymers 90,370-379, (2012).

[41] Fosso-Kankeu, E.; Mittal, H.; Waanders, F.; Ray, S.S.: 2017. Thermodynamic properties and adsorption behaviour of hydrogel nanocomposites for cadmium removal from mine effluents. Journal of Industrial and Engineering Chemistry. **48**, 151-161 (2017).